nature medicine

Human tissue-engineered blood vessels for adult arterial revascularization

Nicolas L'Heureux[1], Nathalie Dusserre[1], Gerhardt Konig[1], Braden Victor[2], Paul Keire[3], Thomas N Wight[3], Nicolas A F Chronos[4], Andrew E Kyles[5], Clare R Gregory[5], Grant Hoyt[6], Robert C Robbins[6] & Todd N McAllister[1]

There is a crucial need for alternatives to native vein or artery for vascular surgery. The clinical efficacy of synthetic, allogeneic or xenogeneic vessels has been limited by thrombosis, rejection, chronic inflammation and poor mechanical properties. Using adult human fibroblasts extracted from skin biopsies harvested from individuals with advanced cardiovascular disease, we constructed tissue-engineered blood vessels (TEBVs) that serve as arterial bypass grafts in long-term animal models. These TEBVs have mechanical properties similar to human blood vessels, without relying upon synthetic or exogenous scaffolding. The TEBVs are antithrombogenic and mechanically stable for 8 months *in vivo*. Histological analysis showed complete tissue integration and formation of vasa vasorum. The endothelium was confluent and positive for von Willebrand factor. A smooth muscle–specific α-actin–positive cell population developed within the TEBV, suggesting regeneration of a vascular media. Electron microscopy showed an endothelial basement membrane, elastogenesis and a complex collagen network. These results indicate that a completely biological and clinically relevant TEBV can be assembled exclusively from an individual's own cells.

Cardiovascular tissue engineering introduced the prospect of a completely biological, living and autologous blood vessel produced *in vitro* to fill the crucial need for functional small-diameter conduits. Since Weinberg and Bell's landmark report[1], the fundamental challenge in the field has been to produce a vessel with sufficient mechanical strength without relying upon permanent synthetic scaffolds. Using animal cells, two of the most promising tissue-engineering models have addressed this challenge[2,3] (other models reviewed in ref. 4). Attempts to transition to human cells, however, underscored the difficulty of producing a clinically relevant conduit. Specifically, these human TEBVs did not provide requisite mechanical strength or required neonatal or juvenile cells[5–8]. Although the use of human cells in low-pressure applications (<20 mmHg) has shown inspiring clinical success in pediatrics[9], the promise of a tissue-engineered graft for adult arterial revascularization remains unrealized[10].

Here we present the first TEBV suitable for autologous small-diameter arterial revascularization in adults. This TEBV was assembled using a new method termed sheet-based tissue engineering. In this approach, fibroblasts are cultured in conditions that promote deposition of extracellular matrix to produce a cohesive sheet that can be detached from the culture flask. These sheets, comprised of living cells and a well-organized endogenous matrix, have probe-burst loads of 883 ± 42 gf and can be layered into three-dimensional tissues or organs with physiological mechanical strength[6,11,12]. This method achieves the goal of completely avoiding the use of exogenous biomaterials. Sheet-based tissue engineering also marks a departure from the dogma of cardiovascular tissue engineering by eliminating the need for smooth muscle cells (SMCs), whose early senescence is associated with decreased burst pressures in human models[7].

RESULTS

TEBV production and short-term *in vivo* implantation

We constructed human age- and risk-matched TEBVs exclusively with cells isolated from individuals who had undergone vascular bypass surgery ($n = 6$, age 65 ± 8 years, range 54–79). Fibroblast sheets were produced in as little as 6 weeks (43 ± 10 μm thick). Sheet thickness increased at a rate of 5 μm/week through 15 weeks. The TEBVs consisted of three components: a living adventitia, a decellularized internal membrane and an endothelium. We assembled the internal membrane by wrapping an 8-week-old fibroblast sheet around a Teflon-coated stainless-steel temporary support tube for three revolutions. After a maturation period of at least 10 weeks, the individual plies fused together to form a homogenous cylindrical tissue. We then dehydrated this tissue to form an acellular substrate for endothelial cell seeding. The internal membrane was also included to provide a barrier against cell migration toward the lumen. We formed the adventitia in a similar fashion, by wrapping a living sheet around the internal membrane. After a second maturation phase, we removed the steel

[1]Cytograft Tissue Engineering, Inc., 3 Hamilton Landing, Suite 220, Novato, California 94949, USA. [2]Capitol Cardiovascular Imaging Center, 1315 Alhambra Boulevard, Suite 320, Sacramento, California 95816, USA. [3]The Hope Heart Program, Benaroya Research Institute at Virginia Mason, 1201 Ninth Avenue, Seattle, Washington 98101, USA. [4]American Cardiovascular Research Institute, 5665 Peachtree Dunwoody Road, Suite 225, Outpatient Center, Atlanta, Georgia 30342, USA. [5]Department of Surgical and Radiological Sciences, School of Veterinary Medicine, University of California Davis, Davis, California 95616, USA. [6]Department of Cardiothoracic Surgery, Falk Cardiovascular Research Center, Stanford University, 300 Pasteur Drive, Stanford, California 94305, USA. Correspondence should be addressed to N.L. (nico@cytograft.com) or T.N.M. (todd@cytograft.com).

Received 11 February 2005; accepted 21 October 2005; published online 19 February 2006; doi:10.1038/nm1364

Table 1 Mechanical properties of age- and risk-matched human TEBVs

Vessel type	Burst pressure (mmHg)	Compliance (percent)[a]	Suture retention (gf)	Wall thickness (μm)
TEBV (4.5 mm internal diameter)	3,468 ± 500 ($n = 5$)	1.5 ± 0.3 ($n = 3$)	162 ± 15 ($n = 9$)	407 ± 49 ($n = 5$)
TEBV (1.5 mm internal diameter)	3,688 ± 1865 ($n = 9$)	ND	ND	200 ± 41 ($n = 3$)
Human saphenous vein	1,680–2,273 refs. 6,18	0.7–1.5 refs.19,20	196 ± 2 ($n = 7$)	~250 refs. 21,22
Human artery	2,031–4,225 ($n = 13$)	4.5–6.2 refs. 19,23,24	200 ± 119 ($n = 9$)	350–710 refs. 25,26

[a]Calculated for a pressure change from 80 to 120 mmHg. ND, not determined.

tube, and seeded endothelial cells in the lumen of the living TEBV. We then subjected the vessel to pulsatile flow that increased from 3 ml/min to 150 ml/min over a 3-d preconditioning period.

TEBVs with an internal diameter of 4.2 mm and a wall thickness of 407 ± 49 μm had mechanical properties that compared favorably with saphenous veins (**Table 1**) and surpassed values reported for any other completely biological TEBV produced *in vitro*[2,7,11,13,14]. We xenografted human TEBVs in an immunosuppressed canine model for short-term evaluation (**Fig. 1**) to confirm that these benchtop mechanical qualities would translate to the surgical setting. The vessels had positive handling characteristics and suturability. At 14 d, histological analysis showed the presence of a massive immune response (data not shown), confirming that only short-term time points can be studied in this xenogeneic model.

Long-term implantation study

We considered two approaches for longer-term *in vivo* evaluation of the TEBV: (i) to develop an autologous animal model or (ii) to implant the human model in an immunodeficient animal. As we (N.L., N.D. & T.N.M., unpublished data) and others have shown that the mechanical properties of TEBV are highly species dependent[2,7], we concluded that the outcome of an autologous animal model was not likely to be representative of the performance of a human TEBV. Therefore, we implanted age- and risk-matched human TEBVs (1.5 mm internal diameter) in nude rats as abdominal interpositional grafts. A pilot group ($n = 13$) received single-layer vessels (without an internal membrane). Overall patency was 85% with time points up to 225 d. Graft diameter, estimated using Doppler-ultrasound imaging, increased over time (data not shown), suggesting the need for increased mechanical strength. A second group ($n = 14$) received two-layer TEBVs (with an internal membrane) to determine whether thicker and stronger vessels would maintain diameter. We explanted 12 patent vessels between 90 and 225 d (86% patency), showing graft incorporation into the surrounding tissue, no blood infiltration in the wall, a smooth lumen, intact anastomoses and no signs of lumen narrowing or aneurysm formation (**Figs. 2** and **3**). Doppler-ultrasound evaluation suggested a stable diameter and we observed no mechanical failures. Overall patency for the two studies was 85%, which, considering the small diameter of the graft and the lack of postoperative antiplatelet therapy, clearly indicates the antithrombogenicity of the TEBV.

Histological analysis of the explanted TEBV at 90 d (**Fig. 2**) showed tissue integration, formation of vasa vasorum and accumulation of cells on the luminal side of the internal membrane. Notably, the internal membrane was largely intact and still acellular. This suggests that the cell-synthesized extracellular matrix does not create an inflammatory response, which has been linked to stenosis[15]. The limited thickness of the 'neomedia' observed in the lumen of the TEBV is consistent with this hypothesis. The neomedia was highly cellular, composed of SMC-specific α-actin–positive cells intertwined with collagen fibers and developing elastic fibers, and was covered by a confluent endothelium (**Fig. 2e–g**). At 6 months, the thicknesses of the neomedia and internal membrane were essentially unchanged (**Fig. 3a–c**). Graft diameter also appeared unchanged, as evidenced by the fact that the initial diameter mismatch to the <1 mm internal diameter abdominal aorta was still visible in the middle of the graft (**Fig. 3d**). As a result of the exclusion of the SMC layer and the lack of immediate contractility, the remodeling to match the diameter of the native artery seems to be a slow process. The increased thickness and number of elastic fibers made the TEBV more closely resemble the native aorta (**Fig. 3c**). Likewise, ultrastructural examination showed cell and extracellular matrix organization that were reminiscent of natural tissues (**Fig. 3e,f**). Although circulating progenitor cells may have participated in the formation of the neomedia, SMCs migrating from the anastomoses were the probable source. Although this remodeling process is unlikely in grafts of clinically relevant length, SMC-specific α-actin–positive cells could be seen at the internal membrane–adventitia interface (**Fig. 2h**). This suggests that SMC-like cells can be recruited from the local environment, as is the case in vasculogenesis, or that implanted fibroblasts have differentiated into myofibroblasts[16]. This recruitment, which increased with time (data not shown), may be a load-induced response as the internal membrane gradually remodels.

Expression of proteoglycan, which is often observed in pathological or developing tissues[17], was seen throughout the TEBV before implantation (**Fig. 2b**). Notably, 90 d after grafting, the TEBV was essentially devoid of proteoglycans, suggesting remodeling into a more physiological tissue (**Fig. 2f**). Similarly,

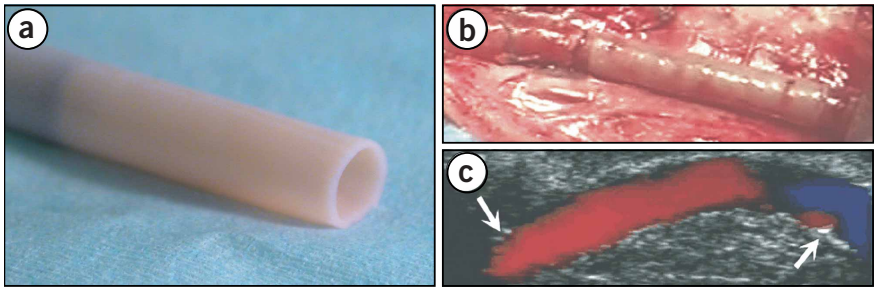

Figure 1 Short-term evaluation of TEBV in canine model. (**a**) Age- and risk-matched TEBV before implantation (4.2 mm internal diameter) being removed from its temporary tubular support. (**b**) TEBV, anastomosed as end-to-end interpositional femoral graft, immediately after removal of the cross-clamps. (**c**) Doppler-ultrasound imaging at 2 weeks shows a patent vessel with uniform lumen and normal flow (arrows indicate anastomoses). TEBVs were endothelialized with autologous canine endothelial cells.

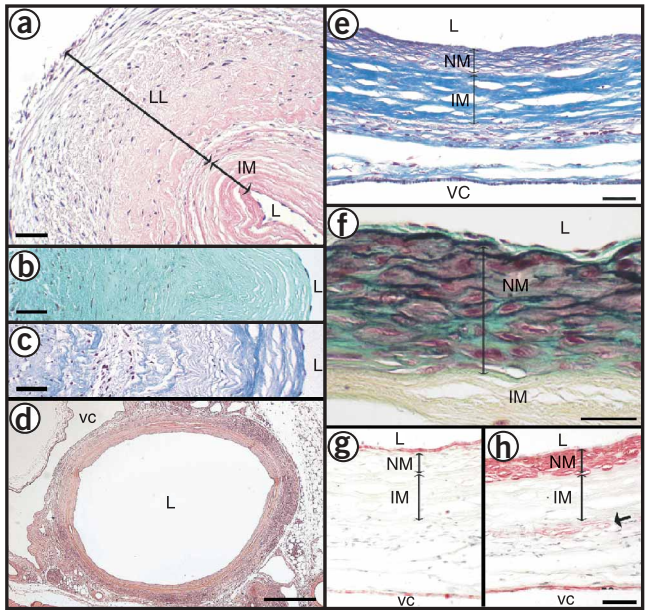

Figure 2 Early remodeling of age- and risk-matched human TEBVs after implantation in athymic rats. (**a**–**c**) Preimplantation histology of a TEBV (1.5 mm internal diameter). (**a**) H&E staining shows a decellularized internal membrane (IM), the living layer (LL) and the lumen (L) of TEBV. Lumens of vessel were seeded with syngeneic rat endothelial cells. The wall is scalloped because this vessel was an unused surgical sample that contracted before fixation. Scale bar, 50 μm. (**b**) Movat staining shows the large proteoglycan (aqua green) content of the TEBV at the time of implantation. Scale bar, 50 μm. (**c**) Verhoff-Masson staining indicates the large collagen content (blue) of the TEBV. Scale bar, 50 μm. (**d**) Ninety days after implantation, H&E staining of the perfusion-fixed graft shows complete tissue integration with minimal inflammatory-immune response and formation of a modest neomedia. VC, vena cava. Scale bar, 500 μm. (**e**) Verhoff-Masson staining indicates that the internal membrane was largely intact and still acellular. The neomedia was rich in collagen and cells and appeared to have elastic fibers (black). Scale bar, 50 μm. (**f**) At higher magnification, Movat staining shows the forming elastic fibers and a developing internal elastic lamella-like structure forming under a confluent endothelium. Proteoglycans were present in the neomedia and subendothelial space but no longer in the internal membrane (yellowish staining indicates collagen). Scale bar, 25 μm. (**g**,**h**) Immunohistochemical staining for von Willebrand factor (**g**) and SMC α-actin (**h**) shows the confluent endothelium and the SMC layers, respectively, of the TEBV and adjacent vena cava. Arrow indicates presence of SMC-specific α-actin–positive cells at the internal membrane–adventitia interface.

proteoglycans that were present in the newly formed neomedia at 90 d (**Fig. 2f**) were absent 3 months later, again suggesting a positive maturation process (**Fig. 3b**).

Primate implantation

Although the small diameter of the rat model created a challenging environment (microsurgery and potential thrombosis), the circumferential wall stress, which is proportional to the diameter, was considerably lower than in clinically relevant TEBVs (3–6 mm internal diameter). To evaluate the TEBV in a more representative biomechanical environment, we implanted age- and risk-matched human TEBVs (4.2 mm internal diameter) as interpositional arterial grafts in three immunosuppressed cynomolgus macaques. We chose this model for its well-defined immunosuppression protocol which is commonly used for xenogeneic transplantation studies. All vessels were patent at explantation ($n = 1$ at 6 weeks and $n = 2$ at 8 weeks). Doppler-ultrasound, computed tomography–angiography (**Fig. 4a**) and necropsy (**Fig. 4b**) confirmed that the vessels were patent with smooth lumens, intact anastomoses and no sign of lumen narrowing or aneurysm formation. Histological observation showed a moderate immune response to the human tissue, limited formation of focal neomedia, formation of vasa vasorum and reendothelialization of an acellular and intact internal membrane (**Fig. 4c**–**f**). Expression of proteoglycan was consistent with that observed in the rat model (**Fig. 4e**), suggesting positive remodeling. Also similar to the rat model, SMC-specific α-actin–positive cells were seen at the internal membrane–adventitia interface (**Fig. 4g**). Moreover, abundant α-actin staining was evident in the perivascular tissue. These observations suggest a possible mechanism for the long-term regeneration of contractile media.

The mechanical requirements for completely biological tissue-engineered grafts are not limited to demonstrating physiological burst pressure and compliance. It is also important that the graft be resistant to rapid degradation and fatigue-induced formation of

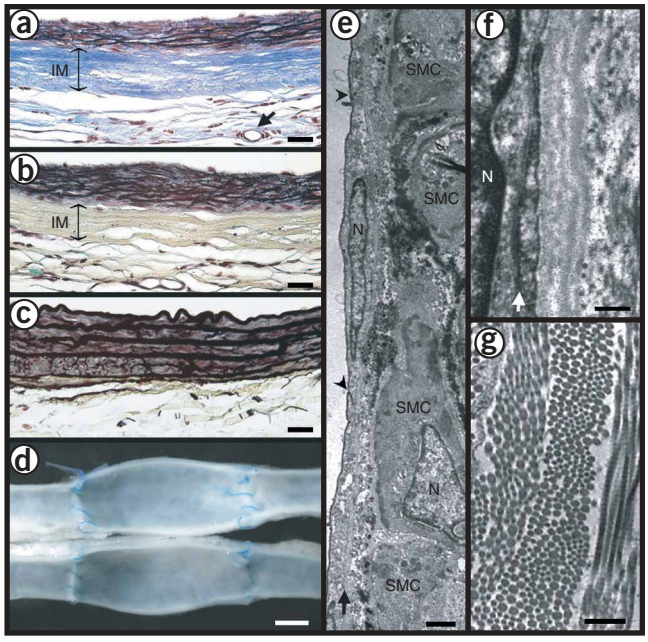

Figure 3 Late remodeling of age- and risk-matched human TEBVs after implantation in athymic rats. (**a**,**b**) After 180 d, Verhoff-Masson (**a**) and Movat (**b**) stainings of the perfusion-fixed TEBV wall showed a largely intact and acellular internal membrane as well as abundant elastic fiber formation in the neomedia. Formation of vasa vasorum was common (arrow in **a**). (**c**) Movat staining of native rat aorta. There is a resemblance with the remodeled wall of the TEBV in **b**. (**d**) At the latest time point (225 d), grafts seemed fully integrated in the surrounding tissue and showed no signs of thrombosis, stenosis or mechanical failure. (**e**–**g**) Transmission electron micrographs. N, nucleus. (**e**) Flat endothelial cells with accompanying basement membrane (arrow) line the lumen of the TEBV. Arrowhead indicates cell-cell junction. Underlying SMCs are rich in microfilaments and dense bodies suggesting a contractile phenotype. The dark staining material along the surface of the SMCs, as shown by ruthenium red, resembles forming elastic fibers. (**f**) Higher magnification of the endothelium shows tight endothelial cell-cell junctions (arrow) and close apposition to a continuous basement membrane. (**g**) Multidirectional bundles of collagen fibers in the internal membrane. A periodic banding pattern typical of collagen fibers is visible.

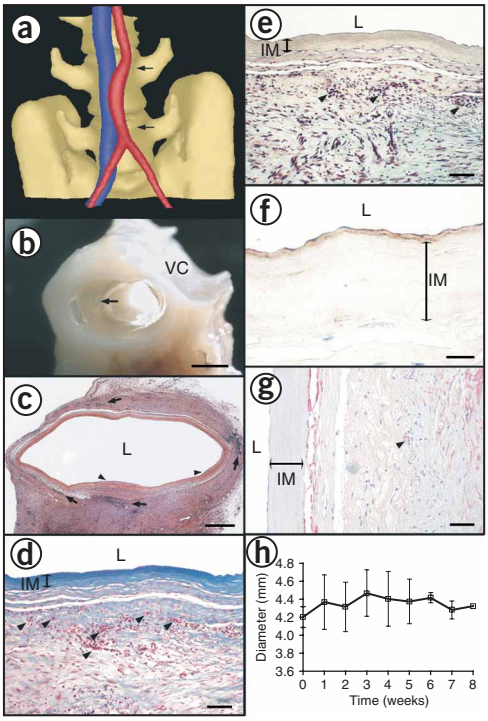

Figure 4 Implantation of age- and risk-matched human TEBV in nonhuman primates. (**a**) Computed tomography angiogram after 8 weeks of implantation showing a patent TEBV (red) and the adjacent vena cava (blue). The initial diameter mismatch is still visible in the middle of the graft and the curved shape is typical of an interpositional graft. (**b**) Perfusion-fixed TEBV at 8 weeks shows complete tissue integration and a smooth lumen with no signs of thrombosis, stenosis or mechanical failure. Arrow indicates suture line. VC, vena cava. (**c**) H&E staining of the graft at 8 weeks shows multiple leukocyte infiltrations (arrows) and rare sites of limited luminal growth (arrowheads). (**d**,**e**) At higher magnification, Verhoff-Masson (**d**) and Movat (**e**) stainings show an intact and still acellular internal membrane. Proteoglycans are effectively absent from the TEBV. Formation of vasa vasorum was noted (arrows in **d**). The substantial immune response observed (arrows in **e**) may be responsible for incomplete tissue integration. (**f**) Immunolabeling for von Willebrand factor shows the confluent endothelium and subendothelial matrix (nuclei counterstained in blue). (**g**) Immunolabeling for SMC-specific α-actin stains a cell population at the internal membrane–adventitia interface (blue counterstain). Arrow indicates small blood vessel. (**h**) TEBV internal diameter was measured at the center of the graft by weekly Doppler-ultrasound examination of all animals. After an increase of about 5% associated with initial pressurization, the diameter remained constant for the duration of the study.

aneurysms *in vivo*. Hence, we followed graft diameter via ultrasound imaging through the course of the primate study (**Fig. 4h**). The constant diameter of the TEBV through 8 weeks indicates that the graft is mechanically stable during the phase of incorporation into the surrounding tissue. These data, coupled with positive histological observations and the absence of aneurysm formation in the long-term rat model, suggest that this TEBV has promise as a clinical graft. Clearly, the key to clinical efficacy will be the long-term remodeling responses in the completely autologous environment. Further xenogeneic or even autologous animal models would offer little insight into this remodeling process in humans. Therefore, autologous TEBVs are currently being evaluated clinically for peripheral arterial revascularization. Although the time to produce these TEBVs (~28 weeks) clearly precludes urgent clinical use, the vast majority of individuals who lack autologous vessels for revascularization can be identified months before surgical intervention. For example, individuals with hemodialysis-dependent end-stage renal disease, with coronary disease and chronic stable angina, or with peripheral vascular disease and claudication follow a well-defined disease progression and can have months-long preoperative waiting periods. Should initial clinical studies prove successful, future efforts will focus on reducing vessel production time and exploring the use of allogeneic TEBVs produced by sheet-based tissue engineering.

METHODS

Tissue culture. We extracted human skin fibroblasts as previously described[6]. For sheet production, we seeded cells at passage 3–5 at 10^4 cells/cm^2 on gelatin-coated T-75 flasks and cultured them in DMEM supplemented with Ham F12 (20%), FetalClone bovine serum (20%), glutamine (2 mM), penicillin (100 U), streptomycin (100 μg/ml) and sodium ascorbate (500 μM). For maturation, we cultured vessels in 45 ml of the same medium, but decreased the concentration of sodium ascorbate to 250 μM. We extracted endothelial cells from saphenous veins and cultured them using endothelial cell growth factor and heparin as previously described[6]. We seeded endothelial cells at 10^5 cells/cm^2 in the TEBV and allowed them to adhere for 3 h. We changed all media three times per week.

Mechanical testing. We determined the mechanical strength of fibroblast sheets ($n = 6$, 8 weeks of culture) using an indentation test. We loaded the center of a circular sheet, mounted on a force transducer, with a spherical tip (9 mm) of a probe at a rate of 20 mm/min until perforation. Force was digitally recorded. Other mechanical testing followed Association for the Advancement of Medical Instruments–American National Standards Institute (ANSI/AAMI) test standard VP20 with minor modifications for biological material. Burst pressure was achieved by increasing hydrostatic pressure within the vessel at a rate of 80 mmHg/min until failure. Pressure was digitally recorded. Clean longitudinal slits were the noted failure mechanism in TEBVs. Human mammary arteries were unused distal segments harvested during bypass surgery or vessels obtained at necropsy. We carefully dissected vessels to expose collaterals for ligation. We tested 3 right internal mammary artery segments and 10 left internal mammary artery segments from eight individuals (age 70 ± 10 years, range 61–87). We separated results into two groups: failures that seemed to be associated with the presence of a collaterals or wall defects (2,031 ± 872, $n = 8$), and high-pressure failures that may reflect maximum material properties (4,225 ± 1368, $n = 5$). To measure suture retention strength, we pulled (2 mm/s) a single throw of 5-0 prolene suture (2.2 ± 0.3-mm bite) through the TEBV segment, which was secured to a force transducer. We digitally recorded force. We obtained samples from the saphenous veins of two individuals, arteries from three individuals (two radial and three internal mammary). We calculated compliance (c) by measuring the change in internal diameter (d) as we varied the pressure (P) at 0.2 Hz between 80 and 120 mmHg. We used high-resolution digital images to determine TEBV outer diameter. The TEBV wall was assumed to be incompressible. Compliance was calculated using the equation:

$$C = \frac{(d_{120} - d_{80})/d_{80}}{\Delta P} \quad (1)$$

Canine studies. We implanted human TEBVs (4.2 mm internal diameter, ~6 cm long) following standard surgical techniques ($n = 5$ grafts in four dogs) using 8-0 prolene. We administered immunosuppressive and antiplatelet therapies starting 48 h before surgery: cyclosporine (7.5 mg/kg), mycophenolate mofetil (20 mg/kg), methyl prednisolone (1 mg/kg per day), acetylsalicylic acid (325 mg per day) and clopidogrel (300 mg initial dose and 75 mg per day after surgery). This protocol was approved by the ethics committee of the Palo Alto Veterans Administration Hospital.

Nude rat studies. We anastomosed human TEBV (1.5 mm internal diameter, ~7 mm long) using 10-0 prolene. In the pilot study (no internal membrane), animals received a single dose of antiplatelet agent (clopidogrel, 30 mg/kg, by mouth) 30 min before surgery. We harvested patent vessels at days 14 ($n = 2$),

30 ($n = 1$), 60 ($n = 1$), 90 ($n = 5$), 180 ($n = 1$) and 225 ($n = 2$). We explanted thrombosed vessels at days 3 ($n = 1$) and 166 ($n = 1$). In the second study (with internal membrane), we did not administer any antiplatelet drugs. We explanted patent vessels at days 90 ($n = 3$), 120 ($n = 2$), 180 ($n = 5$) and 225 ($n = 2$). We explanted thrombosed vessels at days 90 ($n = 1$) and 180 ($n = 1$). This protocol was approved by the Administrative Panel on Laboratory Animal Care of Stanford University.

Primate studies. We implanted human TEBVs (4.2 mm internal diameter, ~3 cm long) using 8-0 prolene as end-to-end iliac ($n = 1$) or abdominal aortic ($n = 2$) interpositional grafts. We administered immunosuppressive and antiplatelet therapies starting 2 d before surgery: cyclosporine A (target plasma level of 250–300 ng/ml until end), mycophenolate mofetil (target plasma level of 1.5–2.0 μg/ml until end), rabbit antithymocyte globulin (5 mg/kg for 5 d), acetylsalicylic acid (10 mg/kg until day 14) and clopidogrel (0.5 mg/kg, until day 4 then wean over 10 d). We explanted patent grafts at 6 weeks (iliac) and 8 weeks (abdominal aorta). This protocol was approved by the Institutional Animal Care and Use Committee of the University of California, Davis and the California National Primate Research Center.

Tissue fixation and histology. We fixed grafts and control vessels *in situ* with cold phosphate-buffered paraformaldehyde 4% after a rinse with cold phosphate saline solution containing 5 mM Ca^{2+}. Animals received heparin before being killed. In rats, we performed whole-body fixation, whereas we fixed only the target vasculature in dogs and primates. Antibodies against SMC α-actin and von Willebrand factor were shown with streptavidin-alkaline phosphatase LSAB 2 system (DakoCytomation #N1584, A0082) and a substrate kit (Vector Labs #SK-5100). We prepared transmission electronic microscopy samples as previously described[6] and further stained them with ruthenium red.

ACKNOWLEDGMENTS

We thank Genzyme Transplant for providing antithymocyte globulin, Roche for providing mycophenolate mofetil (CellSept) and LifeNet for tissue-procurement assistance. We thank M. Haidekker for his help with the image processing of the computed tomography angiogram. This work was supported in part by a grant from the US National Institutes of Health Small Business Innovative Research (2R44HL64462 to N.L.). We thank M.L. Koranski for his help and for performing canine surgeries.

COMPETING INTERESTS STATEMENT

The authors declare competing financial interests (see the *Nature Medicine* website for details).

Published online at http://www.nature.com/naturemedicine/
Reprints and permissions information is available online at http://npg.nature.com/reprintsandpermissions/

1. Weinberg, C.B. & Bell, E. A blood vessel model constructed from collagen and cultured vascular cells. *Science* **231**, 397–400 (1986).
2. Niklason, L.E. *et al.* Functional arteries grown *in vitro*. *Science* **284**, 489–493 (1999).
3. Chue, W.L. *et al.* Dog peritoneal and pleural cavities as bioreactors to grow autologous vascular grafts. *J. Vasc. Surg.* **39**, 859–867 (2004).
4. Kakisis, J.D., Liapis, C.D., Breuer, C. & Sumpio, B.E. Artificial blood vessel: the Holy Grail of peripheral vascular surgery. *J. Vasc. Surg.* **41**, 349–354 (2005).
5. L'Heureux, N., Germain, L., Labbe, R. & Auger, F.A. *In vitro* construction of a human blood vessel from cultured vascular cells: a morphologic study. *J. Vasc. Surg.* **17**, 499–509 (1993).
6. L'Heureux, N., Paquet, S., Labbe, R., Germain, L. & Auger, F.A. A completely biological tissue-engineered human blood vessel. *FASEB J.* **12**, 47–56 (1998).
7. McKee, J.A. *et al.* Human arteries engineered *in vitro*. *EMBO Rep.* **4**, 633–638 (2003).
8. Poh, M. *et al.* Blood vessels engineered from human cells. *Lancet* **365**, 2122–2124 (2005).
9. Shin'oka, T., Imai, Y. & Ikada, Y. Transplantation of a tissue-engineered pulmonary artery. *N. Engl. J. Med.* **344**, 532–533 (2001).
10. Niklason, L.E. Replacement arteries made to order. *Science* **286**, 1493–1494 (1999).
11. L'Heureux, N. *et al.* A human tissue-engineered vascular media: a new model for pharmacological studies of contractile responses. *FASEB J.* **15**, 515–524 (2001).
12. Michel, M. *et al.* Characterization of a new tissue-engineered human skin equivalent with hair. *In Vitro Cell. Dev. Biol. Anim.* **35**, 318–326 (1999).
13. Berglund, J.D., Mohseni, M.M., Nerem, R.M. & Sambanis, A. A biological hybrid model for collagen-based tissue engineered vascular constructs. *Biomaterials* **24**, 1241–1254 (2003).
14. Grenier, G. *et al.* Isolation and culture of the three vascular cell types from a small vein biopsy sample. *In Vitro Cell. Dev. Biol. Anim.* **39**, 131–139 (2003).
15. Davis, C., Fischer, J., Ley, K. & Sarembock, I.J. The role of inflammation in vascular injury and repair. *J. Thromb. Haemost.* **1**, 1699–1709 (2003).
16. Gittenberger-de Groot, A.C., DeRuiter, M.C., Bergwerff, M. & Poelmann, R.E. Smooth muscle cell origin and its relation to heterogeneity in development and disease. *Arterioscler. Thromb. Vasc. Biol.* **19**, 1589–1594 (1999).
17. Wight, T.N. The vascular extracellular matrix. in *Artherosclerosis and Coronary Artery Disease* (eds. Fuster, V., Ross, R. & Topol, E.) 421–440 (Raven Press, New York, 1996).
18. Lamm, P., Juchem, G., Milz, S., Schuffenhauer, M. & Reichart, B. Autologous endothelialized vein allograft: a solution in the search for small-caliber grafts in coronary artery bypass graft operations. *Circulation* **104**, I108–I114 (2001).
19. Dobrin, P.B. Mechanical behavior of vascular smooth muscle in cylindrical segments of arteries *in vitro*. *Ann. Biomed. Eng.* **12**, 497–510 (1984).
20. Cambria, R.P. *et al.* The evolution of morphologic and biomechanical changes in reversed and in-situ vein grafts. *Ann. Surg.* **205**, 167–174 (1987).
21. van der Lugt, A. *et al.* Femorodistal venous bypass evaluated with intravascular ultrasound. *Eur. J. Vasc. Endovasc. Surg.* **9**, 394–402 (1995).
22. Varty, K., Porter, K., Bell, P.R. & London, N.J. Vein morphology and bypass graft stenosis. *Br. J. Surg.* **83**, 1375–1379 (1996).
23. Chamiot-Clerc, P., Copie, X., Renaud, J.F., Safar, M. & Girerd, X. Comparative reactivity and mechanical properties of human isolated internal mammary and radial arteries. *Cardiovasc. Res.* **37**, 811–819 (1998).
24. Girerd, X.J. *et al.* Incompressibility of the human arterial wall: an *in vitro* ultrasound study. *J. Hypertens. Suppl.* **10**, S111–S114 (1992).
25. van Son, J.A., Smedts, F., Vincent, J.G., van Lier, H.J. & Kubat, K. Comparative anatomic studies of various arterial conduits for myocardial revascularization. *J. Thorac. Cardiovasc. Surg.* **99**, 703–707 (1990).
26. van Andel, C.J., Pistecky, P.V. & Borst, C. Mechanical properties of porcine and human arteries: implications for coronary anastomotic connectors. *Ann. Thorac. Surg.* **76**, 58–65 (2003).